

Inhibition of spread of typical bipartite and genuine multiparty entanglement in response to quenched disorder

George Biswas and Anindya Biswas

Department of Physics, National Institute of Technology Sikkim, Ravangla, South Sikkim 737 139, India

Ujjwal Sen

Harish-Chandra Research Institute, HBNI, Chhatnag Road, Jhunsi, Prayagraj 211 019, India

The distribution of entanglement of typical multiparty quantum states is not uniform over the range of the measure utilized for quantifying the entanglement. We intend to find the response of quenched disorder in the state parameters on this non-uniformity for typical states. We find that the typical entanglement, quenched averaged over the disorder, is taken farther away from uniformity, as quantified by decreased standard deviation, in comparison to the clean case. The feature is seemingly generic, as we see it for Gaussian and non-Gaussian disorder distributions, for varying strengths of the disorder, and for disorder insertions in one and several state parameters. The non-Gaussian distributions considered are uniform and Cauchy-Lorentz. Two- and three-qubit pure state Haar-uniform generations are considered for the typical state productions. We also consider noisy versions of the initial states produced in the Haar-uniform generations. A genuine multiparty entanglement monotone is considered for the three-qubit case, while concurrence is used to measure two-qubit entanglement.

I. INTRODUCTION

Random numbers have useful applications in classical information theory, including in cryptography, stochastic estimations, etc. Random quantum states and random unitary operators are the quantum analogs of random numbers in quantum information theory [1–7]. Moreover, random states occur naturally when a quantum system gets measured in an unknown basis, or when the system is perturbed by an uncontrolled and unknown environment. Similarly, random states can also get generated in the initialization of the corresponding quantum devices. Quantum algorithms and other quantum-enabled protocols [8, 9] sometime assume that interaction with environment can somehow be avoided. However, unless an error-correction procedure [8, 9] is incorporated, which can be costly, random states would naturally appear and remain in the corresponding quantum circuits.

In this paper, we investigate entanglement properties [10–12] of randomly generated bipartite and tripartite pure and mixed quantum states, with and without disorder. The case without disorder has, e.g., been considered in [13–23]. We anticipate a situation where noise from the environment, during the preparation of the state for feeding a quantum circuit or during the evolution of the state through the circuit, gathers as disorder in the parameters of the state written as a superposition over the computational basis. Noise typically acts with a preferred basis, and we assume that basis in our case to be the computational basis, which in turn justifies the building up of disorder in the parameters of the state written in that basis. The random bipartite and tripartite states are chosen Haar uniformly. The disorder is inferred as quenched, and assumed to be spread according to Gaussian, uniform, or Cauchy-Lorentz distributions [24].

Quantum entanglement is the existence of states of several separated systems that cannot be created by only local quantum operations and classical communication (LOCC) between the systems [25–27]. There are a large number of measures of entanglement of both bipartite and multiparty quantum states. However, not many of them are computable. We use the concurrence [28, 29] to measure bipartite entanglement and the computable en-

tanglement monotone of Jungnitsch, Moroder, and Gühne (JMG) [30] for measuring genuine multiparticle entanglement. We find that the introduction of quenched disorder in multiparty quantum state parameters generically inhibits the spread of quenched averaged entanglement for typical states of the multiparty systems considered. The considerations are restricted to two- and three-qubit states, of both pure and noisy varieties.

The rest of the paper is arranged as follows. In Sec. II, we briefly discuss the probability distributions from which the random numbers have been chosen and the measures employed to compute quantum entanglement. A short discussion of quenched disorder and quenched averaging is given there. In Sec. III, we discuss the entanglement distributions obtained for bipartite and tripartite Haar-uniformly generated pure states, with and without disorder. Several cases are considered, and are given in separate subsections. Noisy versions of the input states are also used, that lead to mixed states, and these analyses appear in Secs. III B and III F. A conclusion is presented in Sec. IV.

II. GATHERING THE TOOLS

A. Probability density functions

The random numbers utilized to model the disorder, arising in the coefficients of randomly chosen bipartite and tripartite quantum states expressed in the computational basis, have been chosen from Gaussian, uniform, or Cauchy-Lorentz probability distributions. The probability density function for the Gaussian distribution is given by

$$f_G(x) = \frac{1}{\sigma_G \sqrt{2\pi}} e^{-\frac{1}{2} \left(\frac{x-\mu_G}{\sigma_G} \right)^2}, \quad (1)$$

where μ_G is the mean and σ_G is the standard deviation of the distribution. The corresponding semi-interquartile range, which is half of the difference between the third and first quartiles of the distribution function, is given by

$$\gamma_G \approx 0.67448 \times \sigma_G. \quad (2)$$

The probability density function for the uniform distri-

bution is

$$f_U(x) = \begin{cases} \frac{1}{b-a}, & \text{if } a \leq x \leq b, \\ 0, & \text{otherwise.} \end{cases} \quad (3)$$

The mean, standard deviation and semi-interquartile range in this case are given respectively by

$$\mu_U = \frac{b+a}{2}, \quad \sigma_U = \frac{b-a}{2\sqrt{3}}, \quad \text{and} \quad \gamma_U = \frac{b-a}{4}. \quad (4)$$

The probability density function of the uniform distribution in terms of its mean and standard deviation can be written as

$$f_U(x) = \begin{cases} \frac{1}{2\sqrt{3}\sigma_U}, & \text{if } \mu_U - \sqrt{3}\sigma_U \leq x \leq \mu_U + \sqrt{3}\sigma_U, \\ 0, & \text{otherwise.} \end{cases} \quad (5)$$

The Cauchy-Lorentz probability density function is given by

$$f_{C-L}(x|x_0, \gamma_{C-L}) = \frac{\gamma_{C-L}}{\pi [\gamma_{C-L}^2 + (x - x_0)^2]}, \quad (6)$$

where x_0 is the median of the distribution and γ_{C-L} is the scale parameter, being equal to its half width at half maximum or semi-interquartile range. The mean and variance of the Cauchy-Lorentz distribution are not well-defined. The Cauchy principal value of the mean does exist, and equals the median. In absence of the mean, we use the median as a measure of central tendency of the distribution. And in absence of the standard deviation, we use the semi-interquartile range as a measure of dispersion of the distribution. The corresponding cumulative distribution function is

$$\begin{aligned} F_{C-L}(x|x_0, \gamma_{C-L}) &= \int_{-\infty}^x f_{C-L}(x'|x_0, \gamma_{C-L}) dx' \\ &= \frac{1}{\pi} \tan^{-1} \left(\frac{x - x_0}{\gamma_{C-L}} \right) + \frac{1}{2}. \end{aligned} \quad (7)$$

Therefore, the quantile function or the inverse cumulative distribution function is

$$x = x_0 + \gamma_{C-L} \tan \left[\pi \left(F_{C-L} - \frac{1}{2} \right) \right]. \quad (8)$$

This quantile function generates a random number from the Cauchy-Lorentz distribution when F_{C-L} is randomly chosen from a uniform distribution in the range 0 to 1.

B. Entanglement measures

We wish to analyze entanglement in bipartite and tripartite quantum states. The bipartite quantum states that we will encounter are all two-qubit states, and therefore, we can use the concurrence to measure their entanglement contents. Concurrence of a two-qubit density matrix ρ is defined as

$$C(\rho) = \max\{0, \lambda_1 - \lambda_2 - \lambda_3 - \lambda_4\}, \quad (9)$$

where the λ_i 's are square roots of the eigenvalues of $\rho\tilde{\rho}$ in descending order. Here $\tilde{\rho}$ is the spin-flipped ρ : $\tilde{\rho} =$

$(\sigma_y \otimes \sigma_y)\rho^*(\sigma_y \otimes \sigma_y)$, ρ^* is the complex conjugate of ρ in the computational basis [28, 29]. The physical meaning of the concurrence is obtained through its relation, for two-qubit states, with the entanglement of formation [31, 32]. And the entanglement of formation of a bipartite state, not necessarily of two qubits, is a quantifier of the “amount” of singlets necessary to create the state by LOCC.

We now move over to the tripartite case, where we use a computable multiparty entanglement monotone, for both pure and mixed states, given in Ref. [30]. The measure is equal to the negativity [33–38] for the bipartite case, and can be considered to be an extension of negativity to the multipartite case. A tripartite state ρ_{ABC} is not biseparable (i.e., not a convex combination of states which are separable in at least one bipartition) and therefore genuinely multiparty entangled if

$$\rho_{ABC} \neq p_1 \rho_{A|BC}^{\text{sep}} + p_2 \rho_{B|CA}^{\text{sep}} + p_3 \rho_{C|AB}^{\text{sep}}, \quad (10)$$

where $\rho_{A|BC}^{\text{sep}} = \sum_k q_k |\phi_A^k\rangle \langle \phi_A^k| \otimes |\psi_{BC}^k\rangle \langle \psi_{BC}^k|$, etc., and $\{p_i\}$, $\{q_k\}$ are probability distributions. Since any biseparable state is a PPT mixture (i.e., is a convex combination of states that are non-negative under partial transpose (PPT) in at least one bipartition), a state which is not a PPT mixture is necessarily genuine multipartite entangled [33, 34]. Therefore, the state ρ_{ABC} is genuinely multiparty entangled if

$$\rho_{ABC} \neq p_1 \rho_{A|BC}^{\text{ppt}} + p_2 \rho_{B|CA}^{\text{ppt}} + p_3 \rho_{C|AB}^{\text{ppt}}, \quad (11)$$

where $\rho_{A|BC}^{\text{ppt}}$, etc. are states which have a non-negative partial transpose with respect to the indicated bipartition. The genuine entanglement content of this state is characterized and quantified by an entanglement witness W , which is an observable that is non-negative on all biseparable states but has a negative expectation value on at least one entangled state [39]. A witness W is fully decomposable if, for every subset M of a system, it is decomposable with respect to the bipartition given by M and its complement \overline{M} , which implies that there exist positive semidefinite operators P_M and Q_M such that

$$\text{for all } M : W = P_M + Q_M^{T_M}, \quad (12)$$

where T_M is the partial transpose with respect to M . This observable is non-negative on all PPT mixtures, as it is so on all states which are PPT with respect to some bipartition.

Given a multipartite state ρ , if

$$\min \text{Tr}(W\rho) \quad (13)$$

is negative, then ρ is not a PPT mixture, so that it is genuinely multipartite entangled. The negative of the witness expectation value, with the conditions $0 \leq P_M \leq 1$ and $0 \leq Q_M \leq 1$, is defined as the measure of genuine multipartite entanglement. It satisfies the properties of a good entanglement measure [30].

The matlab code for this multipartite entanglement measure which require semi-definite programming [40] has been provided by B. Jungnitsch at [41], and has been used in the calculation of the measure in this work.

C. Quenched disorder and quenched averaging

Disorder can appear in different hues and patterns in a physical system. We consider here a type of disorder that is referred to as “quenched” [42–47]. Within this type of disorder, which is also called “glassy”, the equilibration of the disorder in the system takes a time that is several orders of magnitude higher than the time required to observe the system characteristics which are relevant to our purposes. The system’s physical characteristics, as understood from the values of its physical quantities under consideration, have to be averaged over the disorder to obtain physically meaningful numbers. However, because of the nature of disorder chosen, the averaging needs to be performed only after all physical quantities for given realizations of the disorder have been already calculated. This mode of averaging is referred to as “quenched averaging”.

III. RESPONSE OF BIPARTITE AND TRIPARTITE ENTANGLEMENT TO QUENCHED DISORDER

An arbitrary two-qubit pure state is given by

$$|\psi\rangle = (\alpha_1 + i\alpha_2)|00\rangle + (\beta_1 + i\beta_2)|01\rangle + (\gamma_1 + i\gamma_2)|10\rangle + (\delta_1 + i\delta_2)|11\rangle, \quad (14)$$

where $\alpha_1, \alpha_2, \beta_1, \beta_2, \gamma_1, \gamma_2, \delta_1, \delta_2$ are real numbers, constrained by the normalization condition, $\langle\psi|\psi\rangle = 1$. The state in Eq. (14) can be Haar-uniformly generated by randomly choosing the eight real coefficients from independent normal (Gaussian) distributions of mean $\mu_G = 0$ and standard deviation $\sigma_G = 1$, followed by a normalization. “First step.” A large number (10^7) of such random pure states are generated and the concurrence of each state is calculated. Thus, an entanglement distribution for random two-qubit pure states is obtained, with the range being from 0 till 1. The relative frequency percentages of the distribution for different concurrences is plotted as black asterisks in Fig. 1.

“Second step.” Next, we introduce quenched disorder at α_1 using Gaussian, uniform, or Cauchy-Lorentz distribution functions. One hundred random pure states are generated by choosing random numbers from the Gaussian distribution with $\mu_G = \alpha_1$, where α_1 is the random number generated in the first step, and $\gamma_G = 1/2$. These random numbers are the new α_1 s (in the disordered case), while the other random numbers are the ones selected in the first step, prior to normalization. The random pure states are normalized and their average entanglement calculated. This therefore provides us with another set of 10^7 quenched averaged entanglement values, and again for this distribution, we plot the corresponding relative frequency percentages for different concurrences, as red dots in Fig. 1.

The average entanglement for the Haar-uniformly chosen random pure two qubit states is 0.589, while the corresponding standard deviation is 0.230. This is the clean case, i.e., the case without disorder. It can be seen from Fig. 1 that introduction of disorder in the parameter α_1 from Gaussian distribution does not affect the quenched averaged entanglement (equalling 0.588). However, the quenched averaged standard deviations of the corresponding entanglement distribution is reduced (being 0.197).

We therefore find that the distribution of entanglement of Haar-uniformly chosen quantum states is not uniform in the entire range of possible values, viz. $[0, 1]$, but is concentrated at an intermediate point in $[0, 1]$. Moreover, *introduction of disorder in the parameters of the Haar-uniformly generated quantum states leads to a further concentration of values around an intermediate central value*. This of course has been obtained in a case that is highly specific from several perspectives. *The question that we ask is whether this feature is generic*. To answer this question, we try to remove the specificity of the case studied, viz. checking the response in pure two-party quantum entanglement to Gaussian disorder in a single parameter, from several perspectives.

A. Non-Gaussian disorder

The first of these removals of specificity is effected by considering non-Gaussian disorder distributions. Therefore, the “second step” mentioned above is followed to separately introduce disorder at α_1 from the uniform and Cauchy-Lorentz distributions, instead of the Gaussian one. For the case of the uniform distribution, random numbers are selected from a uniform distribution with $\mu_U = \alpha_1$, where α_1 is the random number generated in the first step, and $\gamma_U = 1/2$. In the Cauchy-Lorentz case, disorder is introduced at α_1 by choosing random numbers from a Cauchy-Lorentz distribution with median $x_0 = \alpha_1$ and semi-interquartile range $\gamma_{C-L} = 1/2$. Note that the mean is equal to the median for the Gaussian and uniform distributions. The data for the uniform distribution is plotted as green crosses, and that for the Cauchy-Lorentz as blue pluses, in Fig. 1.

As already reported above, the average entanglement for the Haar-uniformly chosen random pure two qubit states is 0.589, while the corresponding standard deviation is 0.230, in the ordered (clean) case. All numbers in the calculations for the two-qubit cases are correct to three significant figures. The equality symbols used in the corresponding figures are up to this precision. It can be seen from Fig. 1 that introduction of disorder in the parameter α_1 from Gaussian and uniform distributions does not affect the quenched averaged entanglement (equalling 0.588 in the former case, as already reported above, and 0.589 in the latter one). However, the quenched averaged standard deviations of the corresponding entanglement distributions are reduced (being 0.197 in the case of Gaussian disorder, as already reported above, and 0.205 in the uniform case). There are appreciable changes in both mean and standard deviation (being respectively 0.529 and 0.152) of the entanglement distribution when the disorder in the parameter α_1 is from the Cauchy-Lorentz distribution.

So we find that altering the distribution of disorder does not alter the fact that the quenched disorder results in an inhibition of spread of the entanglement distribution. In fact, moving over to the Cauchy-Lorentz case makes the inhibition significantly more pronounced.

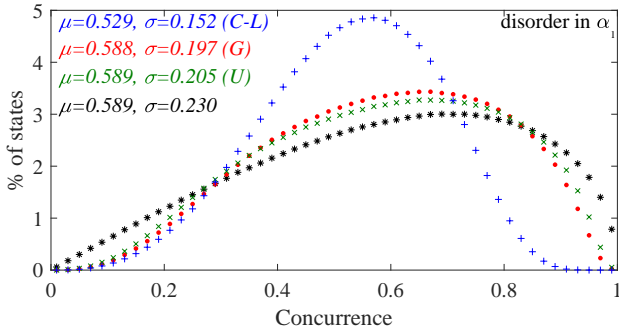


FIG. 1. Inhibition of spread of two-party pure quantum state entanglement in response to quenched disorder. We plot here the percentages (precisely, relative frequency percentages) of Haar-uniformly chosen two-qubit pure states $|\psi\rangle$, given by Eq. (14), with and without disorder at α_1 , against the concurrence values, with the latter ranging between 0 and 1. The black asterisks correspond to percentages of random two-qubit pure states generated Haar uniformly, while the other three curves depict entanglement distributions for random two-qubit pure states with disorder at α_1 chosen from Gaussian (G , red dots), uniform (U , green crosses), and Cauchy-Lorentz ($C - L$, blue pluses) distributions. The quenched averaged values plotted in the figure are for 100 disorder configurations for every α_1 . The figure does not change up to the precision used for averaging over 50 configurations. The initial Haar-uniform generation (in the “first step”) used for the figure utilizes 10^7 states (and hence the same number of α_1 s), although the same plots does not alter, up to the precision used, for 10^6 points. The precision is checked to three significant figures. The calculation of the relative frequency percentages requires a window on the horizontal axis, and it is 0.02 ebits. The convergence checking is done for all other later figures also, but is not explicitly repeated there. The numbers corresponding to the Haar-uniform generation and disorder generation remain the same throughout. The precision and the horizontal axis window are also the same in all figures, except the last two, which relate to three-qubit systems. The vertical axis is dimensionless, while the horizontal one is in ebits, which again is the same in all figures except the last two.

B. Noisy two-qubit states

For two-party pure states, the local von Neumann entropy is a “good” measure of entanglement [31]. And for two-qubit pure states, this is equivalent to the concurrence [28, 29]. We however use concurrence to measure entanglement of two-qubit pure states, to be able to consider the response of disorder on entanglement of two-qubit pure states admixed with noise, thus leading to mixed states, for which, von Neumann entropy of local density matrices does not quantify entanglement, while concurrence does.

The intention in this subsection is to look at the effect, on the response to disorder that we have already seen above, of noise admixture in the states involved. More precisely, we consider a Haar-uniformly generated set of states, $|\psi\rangle$, given by Eq. (14), with each admixed with white noise, so that the actual state is

$$\varrho = p|\psi\rangle\langle\psi| + (1-p)\frac{1}{4}I_4. \quad (15)$$

We consider a fixed p for every $|\psi\rangle$, so that we can assume that we are dealing with a situation where any of the randomly generated states are passing through a fixed noisy

channel, that admixes the input with white noise with a fixed noise level. The state ϱ of course depends on the state $|\psi\rangle$ and the noise parameter p , which are kept silent in the notation. Here, I_4 represents the identity operator on the two-qubit Hilbert space.

We fix attention on the Cauchy-Lorentz disorder distribution, and compare the corresponding quenched averaged entanglement spread in the noisy states with that in the noisy case without disorder. We find that the feature of inhibition of spread remains valid even in this noisy situation. The results are plotted in Fig. 2, where two different values of the noise level, viz. $p = 0.9$ and $p = 0.8$, are considered. Both the mean and standard deviation are affected by the disorder, and in particular for $p = 0.9$, the quenched averaged standard deviation is 0.159, while the standard deviation in the clean case is 0.207. A similar inhibition of the spread is observed for $p = 0.8$, as exhibited in the same figure.

Two points could be mentioned before we move away from this noisy case. Firstly, note that noise itself also leads to an inhibition of the spread.

Secondly, the curves of the percentages of states, when plotted against entanglement (as quantified by concurrence) are non-monotonic. However, in the noiseless cases, all of them have a bell-like shape, and in particular do not have any non-monotonicity near zero entanglement. In the noisy case, there appears an additional non-monotonicity near zero entanglement (in the clean cases). This is not due to any numerical convergence problem, and, e.g., the percentage of zero entanglement states in the clean case for $p = 0.8$ is 2.32%, which remains the same irrespective of whether 10^7 or 10^6 states are considered in the Haar-uniform generation, up to three significant figures. This additional non-monotonicity near zero entanglement can be expected from the fact that the noise inflicted has brought the original set of states closer to the separable ball, and has resulted in more states clustered near the zero-entanglement point. We will come back to this point again when we consider noisy three-qubit states below, where this additional non-monotonicity will be absent. Note that the percentage of zero entanglement states decreases with increasing p , as expected. Note that increasing p corresponds to decrease in noise. Note also that this additional non-monotonicity does not remain in the disordered case, due to the smearing-out effect of the quenched averaging process.

C. Disorder in multiple parameters

We revert to pure states, but now consider disorder in multiple parameters. Note that in the considerations until now, we have analyzed situations where there is disorder only in one parameter of the Haar-uniformly generated state, $|\psi\rangle$, in Eq. (14).

1. Two parameters

We now analyze the situation where disorder is introduced in two parameters, viz. α_1 and β_1 , independently from Gaussian, uniform, or Cauchy-Lorentz distributions. Random numbers are selected from Gaussian, uniform dis-

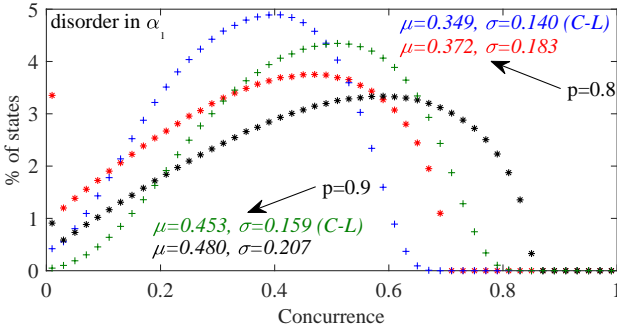


FIG. 2. Effect of noise on the inhibited spread of two-party entanglement due to disorder insertion. The considerations in this figure are the same as in the preceding one, except that only the Cauchy-Lorentz disorder is considered, and that the states are admixed with white noise. The symbols are also different in this figure as compared to the preceding one. The black asterisks and the green pluses depict the case when noise-level is given by $p = 0.9$, with the dots being for the clean case and the pluses for the quenched-averaged situation. The red asterisks and the blue pluses are similarly for $p = 0.8$. For a discussion on the additional non-monotonicity near zero entanglement that occurs in this noisy case for the curves corresponding to the clean situations, see text.

tributions with $\mu_{G/U} = \alpha_1$, $\gamma_{G/U} = 1/2$ and $\mu_{G/U} = \beta_1$, $\gamma_{G/U} = 1/2$, while random numbers are chosen from Cauchy-Lorentz distributions with $x_0 = \alpha_1$, $\gamma_{C-L} = 1/2$ and $x_0 = \beta_1$, $\gamma_{C-L} = 1/2$. These random numbers are the new α_1 s and β_1 s in Eq. (14), while the other random numbers are the ones selected in the first step, prior to normalization. One hundred such pure states are generated and the average entanglement with disorder is calculated. The resulting entanglement distributions are plotted in Fig. 3. It can be seen from Fig. 3 that introduction of disorder in

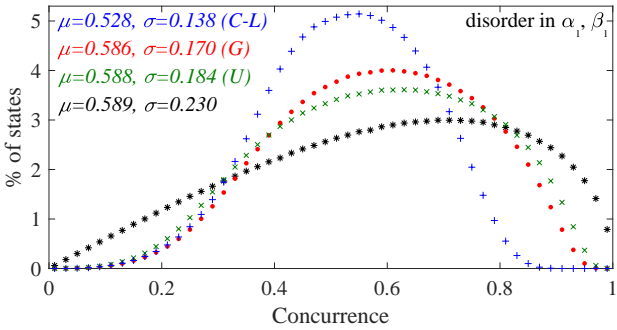


FIG. 3. Further hindrance to entanglement spread as we introduce disorder in more parameters. The case of introducing disorder in two parameters is considered in this figure, while the case of doing the same for four parameters is considered in the succeeding figure. The considerations are the same as in Fig. 1, except that the disorder is introduced in α_1 and β_1 , instead of just α_1 .

both the parameters α_1 and β_1 from Gaussian and uniform distributions does not affect the average entanglement appreciably (being 0.586 in the Gaussian case and 0.588 in the uniform one). However, the standard deviations of the corresponding entanglement distributions are reduced further (being 0.170 in the Gaussian case and 0.184 in the uniform one) in comparison with the matching cases where disorder was introduced in the coefficient α_1 only. There are appreciable changes in both mean and standard devi-

ation (being respectively 0.528 and 0.138) of the entanglement distributions when the disorders in the parameters α_1 and β_1 are randomly chosen from the Cauchy-Lorentz distribution, and again the standard deviation is lower than when a Cauchy-Lorentz disorder was inserted only in the parameter α_1 (compare with Fig. 1).

2. Four parameters

We have already seen that introducing disorder in two parameters leads to increased restriction, in comparison to when we introduce the same in one parameter, on the spread of entanglement on the span $[0, 1]$. Does this increase in restriction to spread continue when we introduce disorder in even further parameters? In an attempt to find this answer, we now consider the effect of introducing disorder in four parameters.

Therefore, we now introduce disorder in the parameters α_1 , β_1 , γ_1 , and δ_1 independently from Gaussian, uniform, or Cauchy-Lorentz distributions. Random numbers for introduction of disorder are selected from Gaussian or uniform distributions with

$$\begin{aligned} \mu_{G/U} &= \alpha_1, \gamma_{G/U} = 1/2, \\ \mu_{G/U} &= \beta_1, \gamma_{G/U} = 1/2, \\ \mu_{G/U} &= \gamma_1, \gamma_{G/U} = 1/2, \\ \mu_{G/U} &= \delta_1, \gamma_{G/U} = 1/2, \end{aligned}$$

while random numbers are chosen from Cauchy-Lorentz distributions with

$$\begin{aligned} x_0 &= \alpha_1, \gamma_{C-L} = 1/2, \\ x_0 &= \beta_1, \gamma_{C-L} = 1/2, \\ x_0 &= \gamma_1, \gamma_{C-L} = 1/2, \\ x_0 &= \delta_1, \gamma_{C-L} = 1/2. \end{aligned}$$

These random numbers are the new α_1 s, β_1 s, γ_1 s, and δ_1 s, while the other random numbers are the ones selected in the first step, prior to normalization. Once more, one hundred such pure states are generated and the quenched averaged entanglement is calculated. The resulting entanglement distributions are plotted in Fig. 4. It can be seen

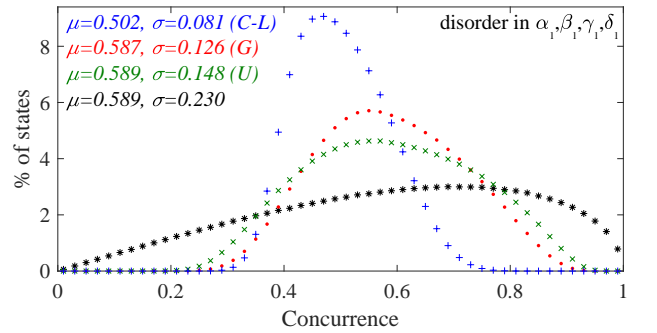


FIG. 4. Disorder in four parameters lead to increased restriction, in comparison to the case when disorder was introduced in two parameters, in spread of entanglement in two-qubit states. All considerations except the increased number of parameters is the same as in the preceding figure.

from Fig. 4 that introduction of disorder in the four parameters α_1 , β_1 , γ_1 , and δ_1 from Gaussian or uniform

distributions again does not appreciably affect the average entanglement (being 0.587 in the Gaussian case and 0.589 in the uniform case) with respect to its value in the clean case. However, the standard deviations of the corresponding entanglement distributions are reduced further than their values in the case when disorder was introduced in two parameters, which themselves were lower than the clean case value. Specifically, the standard deviations are 0.126 and 0.148, respectively for introduction of Gaussian and uniform quenched disorders. There are considerable decreases in both the mean and standard deviation (respectively, 0.502 and 0.081) of the entanglement distributions when the disorder in the parameters α_1 , β_1 , γ_1 , and δ_1 are randomly and independently chosen from the Cauchy-Lorentz distribution.

D. Effect of variation in dispersion of disorder

We revert to disorder in a single parameter, but stay with pure states. The dispersion, as quantified by the semi-interquartile range, has until now been kept fixed at $1/2$, and which we wish to vary now to see its effect on the inhibition of spread of entanglement. Changing the semi-interquartile range can be interpreted as varying the strength of the disorder introduced, with increase of semi-interquartile range implying increase of the strength. We fix attention on the Gaussian disorder for this purpose, and also introduce the disorder only on a single parameter. Random numbers are selected from Gaussian distributions with $\mu_G = \alpha_1$, and γ_G varying from 0.3 to 0.7 at intervals of 0.1. These random numbers are the new α_1 s in Eq. (14), while the other random numbers are the ones selected in the first step, prior to normalization. Just like in the other cases, one hundred such pure states are generated with the disorder being chosen from the Gaussian distribution, and then the average entanglement is calculated. The resulting entanglement distributions (for different semi-interquartile ranges) are plotted in Fig. 5. It can

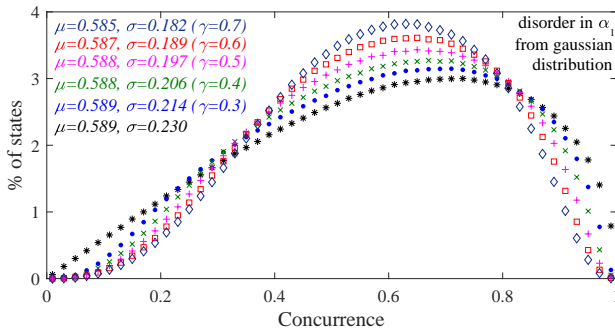


FIG. 5. Effect of variation of strength of disorder. The considerations are the same as in Fig. 1, except that only the Gaussian disorder is considered, and that different semi-interquartile ranges are used for the plots. The symbols are also different here. Black asterisks represent the case when there is no disorder, and has appeared in several figures before, including Fig. 1. The curve with pink pluses is for $\gamma_G = 1/2$, and was also present in Fig. 1. The blue (cyan) dots, green crosses, red squares, and blue-black diamonds are respectively for $\gamma_G = 0.3, 0.4, 0.6$, and 0.7 . Note that the suffix of γ_G is kept silent in the figure legend on the plot.

be seen from Fig. 5 that the average entanglement remains

almost unchanged with the variation of γ_G , while the standard deviation of the entanglement distributions decreases with the increase of γ_G . therefore, as the strength of disorder in the states increases, the standard deviation of the resulting entanglement distributions decreases. This feature can help us understand the reason why the Cauchy-Lorentz distribution has consistently been found to lead to greater inhibition of the spread of entanglement in the previous cases, whenever compared with Gaussian and uniform disorder distributions with same semi-interquartile ranges. The Gaussian and uniform distributions have a finite mean, unlike the Cauchy-Lorentz distribution. For two probability distributions (among Gaussian, uniform, and Cauchy-Lorentz) having the same semi-interquartile range, but with one having a finite mean and the other without, we can say that the latter has a longer “reach” in its domain of definition, viz. the real line, that has led to the non-existence of the mean ($\int_{-\infty}^{+\infty} f(x)dx$ exists and is finite, but $\int_{-\infty}^{+\infty} xf(x)dx$ does not exist, for a probability density $f(x)$ on the real line). And consequently, we can interpret that the latter has a higher dispersion (spread), even though it has the same semi-interquartile range as the former.

E. Three-qubit pure states

We now move over to the three-qubit case, considering pure states in this subsection. The succeeding subsection deals with noisy (mixed) three-qubit states. The entanglement measure considered in both this and the succeeding sections is the JMG entanglement monotone. A three-qubit random pure state can be represented as

$$|\Psi\rangle = (a_1 + ia_2)|000\rangle + (b_1 + ib_2)|001\rangle + (c_1 + ic_2)|010\rangle + (d_1 + id_2)|011\rangle + (e_1 + ie_2)|100\rangle + (f_1 + if_2)|101\rangle + (g_1 + ig_2)|110\rangle + (h_1 + ih_2)|111\rangle. \quad (16)$$

where $a_1, a_2, b_1, b_2, c_1, c_2, d_1, d_2, e_1, e_2, f_1, f_2, g_1, g_2, h_1, h_2$ are real numbers, constrained by the normalization condition, $\langle \Psi | \Psi \rangle = 1$. The state in Eq. (16) can be Haar-uniformly generated by randomly choosing the sixteen real coefficients from independent normal distributions of vanishing mean and unit standard deviation, followed by a normalization. A large number (2×10^4) of such random pure states are generated, normalized, and the entanglement monotone of each state is calculated. Next, we introduce disorder at a_1, b_1, c_1 , and d_1 , independently from Gaussian, uniform, or Cauchy-Lorentz distribution functions. The disorder is introduced by choosing random numbers from Gaussian and uniform distributions with

$$\begin{aligned} \mu_{G/U} &= a_1, \gamma_{G/U} = 1/2, \\ \mu_{G/U} &= b_1, \gamma_{G/U} = 1/2, \\ \mu_{G/U} &= c_1, \gamma_{G/U} = 1/2, \\ \mu_{G/U} &= d_1, \gamma_{G/U} = 1/2, \end{aligned}$$

where a_1, b_1, c_1 , and d_1 are the random numbers generated in the first step. Cauchy-Lorentz distributions with

$$\begin{aligned} x_0 &= a_1, \gamma_{C-L} = 1/2, \\ x_0 &= b_1, \gamma_{C-L} = 1/2, \\ x_0 &= c_1, \gamma_{C-L} = 1/2, \\ x_0 &= d_1, \gamma_{C-L} = 1/2, \end{aligned}$$

are also used to introduce disorders at a_1, b_1, c_1 , and d_1 . These random numbers are the new a_1, b_1, c_1 , and d_1 , while the other random numbers are the ones selected in the first step, prior to normalization. For every set of values of a_1, b_1, c_1 , and d_1 , chosen in the first step, fifty disordered states are generated by employing the above mentioned procedure. The random pure states are normalized and their average entanglement (the quenched averaged JMG entanglement monotone) calculated. The resulting entanglement distributions are plotted in Fig. 6. It can

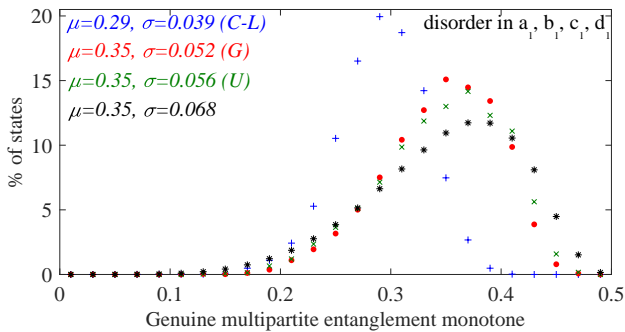


FIG. 6. Inhibition of spread of entanglement in the pure three-qubit state space due to insertion of disorder in state parameters. We plot here the relative frequency percentages of Haar-uniformly generated random three-qubit pure states (with and without disorder at a_1, b_1, c_1, d_1) against the JMG entanglement monotone, with the latter ranging between 0 and 1/2. The black asterisks correspond to percentage of random three-qubit pure states generated Haar uniformly, while the other three curves depict entanglement distributions for random three-qubit pure states with disorder at a_1, b_1, c_1, d_1 chosen from Gaussian (G , red dots), uniform (U , green crosses), or Cauchy-Lorentz ($C-L$, blue pluses) distributions. The numbers in this figure and the succeeding one are correct to two significant figures. The window of the entanglement monotone used for calculating the percentages is 0.02. Both axes represent dimensionless quantities.

be seen from Fig. 6 that the average entanglement of random three-qubit pure states chosen Haar uniformly is 0.35, while the standard deviation of the entanglement distribution is 0.068. The average entanglement remains constant when disorders are introduced in the coefficients a_1, b_1, c_1 , and d_1 from the Gaussian or uniform distributions (being 0.35 for both the cases), while the standard deviations for the entanglement distributions of disordered states are reduced (to 0.052 for the Gaussian case and 0.056 for the uniform one) in comparison to that in the clean case. The average as well as the standard deviation of the entanglement distribution are reduced (to 0.29 and 0.039 respectively) when disorder is introduced in the coefficients a_1, b_1, c_1 , and d_1 from the Cauchy-Lorentz distribution.

F. Noisy three-qubit states

One could have used simpler measures to quantify genuine multiparty entanglement, if we were required to deal with only pure three-qubit states. An example of such a measure is the generalized geometric measure [48–54]. We have however chosen to work with the JMG entanglement monotone due to its tractability for mixed multiparty states, to be considered in this subsection.

Indeed, in this subsection, we wish to investigate the effect of noise on the restriction of spread of the JMG entanglement monotone in the space of three-qubit states. Precisely, we consider the state

$$\tilde{\rho} = p|\Psi\rangle\langle\Psi| + (1-p)\frac{1}{8}I_8, \quad (17)$$

for every $|\Psi\rangle$ (see Eq. (16)) generated in the clean or the disordered cases. Here, I_8 is the identity operator on the three-qubit Hilbert space. This is exactly similar to the analysis in Sec. IIIB, except that we are considering three-qubit states now, and the measure is the JMG entanglement monotone. The effect obtained is again very similar, viz. noise leads to further inhibition of the spread of entanglement. The details of the numerical simulations are presented in Fig. 7. We have focused attention only on the Cauchy-Lorentz disorder. Just like for the two-qubit case, noise restricts the spread of entanglement even in the clean cases.

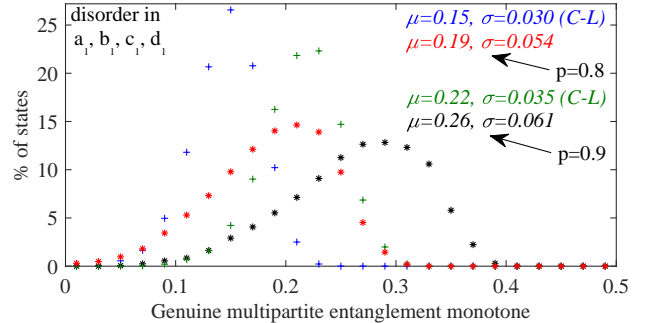


FIG. 7. Further disorder-induced inhibition to spread of entanglement of three-qubit states in presence of noise. The considerations are exactly the same as in the preceding figure, except that the states are admixed with white noise, and that only Cauchy-Lorentz disorder is considered. The noise levels considered are given by $p = 0.9$ and $p = 0.8$. For $p = 0.9$, the black asterisks and green pluses represent the clean and disorder-averaged cases respectively. And for $p = 0.8$, the corresponding symbols are respectively red asterisks and blue pluses.

IV. CONCLUSION

We have analyzed the response to introduction of quenched disorder in multiparty quantum state parameters on the entanglement in those states. We have considered two-qubit and three-qubit states in the analysis, with the entanglement measure considered for two-qubit states being the concurrence and that for three-qubit states being the Jungnitsch-Moroder-Guhne genuine multiparty entanglement monotone. The relative frequency percentages of states for given (small) windows of entanglement are not

uniform for all ranges of the entanglements. We measured this non-uniformity by the standard deviation of the entanglement distribution of these percentages. We found that insertion of disorder in the state parameters generically shrinks the standard deviation from its clean-case value (i.e., value in the corresponding case without disorder).

We began with Gaussian disorder in a single state parameter for two-qubit pure states, and found that the distribution of the quenched-averaged entanglements has a lower standard deviation than the clean case. We then removed the specificities in this case in several ways. We considered non-Gaussian cases, viz. when disorder is introduced by using the uniform distribution as well as that using the Cauchy-Lorentz one, where the latter one is different from the Gaussian and uniform distributions in that it does not have a mean. The Cauchy-Lorentz distribution turned out to be the one that provided the most hindrance to the spread of entanglement. We also considered the case when disorder is introduced in several state parameters, with more hindrance obtained as we increased the number of parameters in which disorder is inserted. We also found that increasing the strength of the disorder increases the localization effect on the entanglement spread.

We also considered the response of disorder introduction in parameters of three-qubit pure states, and found that the inhibition of the spread of entanglement - genuine multiparty entanglement in this case - can again be seen in this case. For both two- and three-qubit cases, we consid-

ered the effect of noise on the phenomenon of inhibition of spread of entanglement in response to disorder introduction.

Why does an entanglement measure that is allowed to span over a certain range does not cover that uniformly? The answer could be because the physical characteristic, viz. entanglement, is a nonlinear function of the state parameters. A peak develops in the allowed range of entanglement, when random quantum states are chosen. The distribution therefore has an average, and a nontrivial spread. It may intuitively seem that if we “rattle” the state parameters, the distribution of the entanglement will also be rattled: the mean will change and the spread will increase. What we saw is that while the mean does often change, the exact opposite happens for the spread: it decreases. Moreover, the stronger the rattling, the stronger is the decrease in spread. We believe that the results will be of importance for considerations in quantum technologies as well as for understanding the black hole information paradox.

ACKNOWLEDGMENTS

US acknowledges support from the Department of Science and Technology, Government of India through the QuEST grant (grant number DST/ICPS/QUEST/Theme-3/2019/120).

[1] J. Emerson, Y. S. Weinstein, M. Saraceno, S. Lloyd, and D. G. Cory, *Science* **302**, 2098 (2003).

[2] A. Harrow, P. Hayden, and D. Leung, *Phys. Rev. Lett.* **92**, 187901 (2004).

[3] P. Hayden, D. Leung, P. W. Shor, and A. Winter, *Communications in Mathematical Physics* **250**, 371 (2004).

[4] B. H. Clowers, M. E. Belov, D. C. Prior, W. F. Danielson, Y. Ibrahim, and R. D. Smith, *Analytical Chemistry* **80**, 2464 (2008).

[5] X. Ma, X. Yuan, Z. Cao, B. Qi, and Z. Zhang, *npj Quantum Information* **2**, 16021 (2016).

[6] N. J. Russell, L. Chakhmakhchyan, J. L. O’Brien, and A. Laing, *New Journal of Physics* **19**, 033007 (2017).

[7] G. Muraleedharan, A. Miyake, and I. H. Deutsch, *New Journal of Physics* **21**, 055003 (2019).

[8] J. Preskill, *Lecture notes for Physics 219: Quantum computation*

[9] M. A. Nielsen and I. L. Chuang, *Quantum Computation and Quantum Information: 10th Anniversary Edition* (Cambridge University Press, 2010).

[10] R. Horodecki, P. Horodecki, M. Horodecki, and K. Horodecki, *Rev. Mod. Phys.* **81**, 865 (2009).

[11] O. Gühne and G. Tóth, *Physics Reports* **474**, 1 (2009).

[12] S. Das, T. Chanda, M. Lewenstein, A. Sanpera, A. Sen De, and U. Sen, “The separability versus entanglement problem,” in *Quantum Information* (John Wiley and Sons, Ltd, 2016) Chap. 8, pp. 127–174.

[13] D. N. Page, *Phys. Rev. Lett.* **71**, 1291 (1993).

[14] S. K. Foong and S. Kanno, *Phys. Rev. Lett.* **72**, 1148 (1994).

[15] S. Sen, *Phys. Rev. Lett.* **77**, 1 (1996).

[16] G. Smith and D. Leung, *Phys. Rev. A* **74**, 062314 (2006).

[17] O. C. O. Dahlsten, R. Oliveira, and M. B. Plenio, *Journal of Physics A: Mathematical and Theoretical* **40**, 8081 (2007).

[18] A. Serafini, O. C. O. Dahlsten, D. Gross, and M. B. Plenio, *Journal of Physics A: Mathematical and Theoretical* **40**, 9551 (2007).

[19] Y. Nakata and M. Murao, *Phys. Rev. A* **84**, 052321 (2011).

[20] M. P. Müller, O. C. O. Dahlsten, and V. Vedral, *Communications in Mathematical Physics* **316**, 441 (2012).

[21] F. Deelan Cunden, P. Facchi, G. Florio, and S. Pascazio, *The European Physical Journal Plus* **128**, 48 (2013).

[22] O. C. O. Dahlsten, C. Lupo, S. Mancini, and A. Serafini, *Journal of Physics A: Mathematical and Theoretical* **47**, 363001 (2014).

[23] M. Fukuda and R. Koenig, *Journal of Mathematical Physics* **60**, 112203 (2019).

[24] J. Gentle, W. K. Härdle, and Y. Mori, *Handbook of Computational Statistics: Concepts and Methods* (Springer-Verlag Berlin Heidelberg, 2012).

[25] A. Einstein, B. Podolsky, and N. Rosen, *Phys. Rev.* **47**, 777 (1935).

[26] E. Schrödinger, *Mathematical Proceedings of the Cambridge Philosophical Society* **31**, 555 (1935).

[27] R. F. Werner, *Phys. Rev. A* **40**, 4277 (1989).

[28] D. Deutsch, *Phys. Rev. Lett.* **78**, 5022 (1997).

[29] W. K. Wootters, *Phys. Rev. Lett.* **80**, 2245 (1998).

[30] B. Jungnitsch, T. Moroder, and O. Gühne, *Phys. Rev. Lett.* **106**, 190502 (2011).

[31] C. H. Bennett, H. J. Bernstein, S. Popescu, and B. Schumacher, *Phys. Rev. A* **53**, 2046 (1996).

[32] C. H. Bennett, D. P. DiVincenzo, J. A. Smolin, and W. K. Wootters, *Phys. Rev. A* **54**, 3824 (1996).

[33] A. Peres, *Phys. Rev. Lett.* **77**, 1413 (1996).

[34] M. Horodecki, P. Horodecki, and R. Horodecki, *Physics Letters A* **223**, 1 (1996).

[35] K. Życzkowski, P. Horodecki, A. Sanpera, and M. Lewenstein, *Phys. Rev. A* **58**, 883 (1998).

[36] J. Lee, M. S. Kim, Y. J. Park, and S. Lee, *Journal of Modern Optics* **47**, 2151 (2000).

[37] G. Vidal and R. F. Werner, *Phys. Rev. A* **65**, 032314 (2002).

[38] M. B. Plenio, *Phys. Rev. Lett.* **95**, 090503 (2005).

[39] D. Chruściński and G. Sarbicki, *Journal of Physics A: Mathematical and Theoretical* **47**, 483001 [40] L. Vandenbergh and S. Boyd, *SIAM Review* **38**, 49 (1996).

[41] B. Jungnitsch, “Pptmixer: A tool to detect genuine multipartite entanglement,” <http://www.mathworks.com/matlabcentral/fileexchange/10021253> (2010).

[42] D. Chowdhury, *Spin Glasses and Other Frustrated Systems* (World Scientific, 1986).

[43] M. Mezard, G. Parisi, and M. Virasoro, *Spin Glass Theory and Beyond* (World Scientific, 1986).

[44] B. K. Chakrabarti, A. Dutta, and P. Sen, *Quantum Ising Phases and Transitions in Transverse Ising Models* [45] H. Nishimori, *Statistical Physics of Spin Glasses and Information* (Oxford University Press, Oxford; New York, 2001).

[46] S. Sachdev, *Quantum Phase Transitions*, 2nd ed. (Cambridge University Press, 2011).

[47] S. Suzuki, J. Inoue, and B. K. Chakrabarti, *Quantum Ising Phases and Transitions in Transverse Ising Models*, 2nd ed. (Springer-Verlag Berlin Heidelberg, 2013).

[48] A. Sen(De) and U. Sen, *Phys. Rev. A* **81**, 012308 (2010).

[49] A. S. De and U. Sen, [arXiv:1002.1253](https://arxiv.org/abs/1002.1253) (2010).

[50] A. Biswas, R. Prabhu, A. Sen(De), and U. Sen, *Phys. Rev. A* **90**, 032301 (2014).

[51] T. Das, S. S. Roy, S. Bagchi, A. Misra, A. Sen(De), and U. Sen, *Phys. Rev. A* **94**, 022336 (2016).

[52] A. Shimony, *Annals of the New York Academy of Sciences* **755**, 675 (1995).

[53] T.-C. Wei and P. M. Goldbart, *Phys. Rev. A* **68**, 042307 (2003).

[54] M. Bisognano, F. Dell’Antonio, S. De Siena, and F. Illuminati, *Phys. Rev. A* **77**, 062304 (2008).